Nonlinear System Identification Based on Convolutional Neural Networks for Multiple Drug Interactions

Koji Kashihara, *Member, IEEE*

***Abstract*—In heart failure patients, hemodynamics can be regulated by therapeutic drugs. Although the cardiovascular responses to these drugs usually include nonlinearity and drug interactions, it is difficult to identify the characteristics of the dynamics under such conditions. This study, therefore, was aimed at evaluating the technique used for nonlinear system identification based on convolutional neural networks (CNN). As an image (i.e., pixel values corresponding to time-course data), CNN can be used to treat the complicated relation between previous inputs (i.e., drug infusions) and outputs (i.e., hemodynamics). To compare the accuracy of CNN, traditional methods based on the standard neural networks (NN) and fast Fourier transformation (FFT) were applied to nonlinear system identification with drug interactions. The cardiac output and arterial blood pressure under heart failure were modulated by the drug infusions of an inotropic agent and a vasodilator. CNN accurately predicted the dynamic system responses regardless of the inclusion of nonlinearity and drug interactions. Based on the findings of this study, CNN to carry out nonlinear system identification could clarify complicated pharmacodynamics, and thus could be useful for in appropriate cardiac treatment with multiple therapeutic agents.**

I. Introduction

Hemodynamic conditions in cardiac patients can be controlled by multiple infusions of therapeutic drugs, such as an inotropic agent and a vasodilator. Inotropic agents (e.g., dobutamine: DB) can increase the force and velocity of cardiac muscle contraction and enhance cardiac output (CO) [1]. Vasodilators (e.g., sodium nitroprusside: SN) can reduce systemic vascular resistance and promote the attenuation of the afterload on the heart. These actions make it possible to decrease arterial blood pressure (AP) and increase stroke volume [2],[3].

To complete the treatment of cardiac patients, it is crucial to understand the pharmacodynamics during multiple drug infusions. In particular, patients with heart failure may have nonlinear and time-variant responses under drug interactions with disturbances. For example, a multivariable drug-delivery system can regulate the hemodynamics (e.g., CO, AP, and heart rates) in heart failure patients by using an inotropic agent and a vasodilator [4],[5]. However, it is difficult to identify a nonlinear dynamic system with interactions during multiple drug infusions.

Standard neural networks (NN) are a simple tool used to clarify nonlinear responses [6],[7]. NN-based controllers have showed high performance, regardless of unexpected drug responses in heart failure [8],[9]. However, a more accurate method is needed to identify the pharmacodynamics of multiple drug infusions, which would be linked to advanced treatment technologies for cardiac patients.

Convolutional NN (CNN) [10] may become an efficient tool for estimating the pharmacodynamics of nonlinearity and drug interactions. The CNN structure consists is composed of convolutional layers and fully connected layers corresponding to NN. Compared to traditional methods, CNN have shown accurate results in classifying image categories [10]. However, a technique for dynamic system identification (i.e., the time-course analysis of input/output history) based on CNN has not been sufficiently established. This study, therefore, was aimed at evaluating the accuracy of the existing method used for nonlinear system identification by using CNN and comparing it with the results of traditional methods, such as the NN and fast Fourier transformation (FFT).

II. Modeling of Pharmacodynamics

A. *Dataset*

Mathematical models for drug responses were created from the dataset [9] in anesthetized and artificially ventilated dogs with acute heart failure. CO and AP responses for 10 min were recorded at a 10-Hz sampling rate. The step responses of ΔCO and ΔAP (i.e., CO and AP changed from the baseline values after heart failure) during DB and SN infusions were averaged every 30 s.

B. *Drug Responses*

In the cascade model, pharmacodynamics can be shown as a linear first-order transfer function and a sigmoidal function to express nonlinearity [9]. Single-input single-output response [$\Delta\tilde{o}(t)$] (i.e., DB-CO, DB-AP, SN-CO, or SN-AP loop) was described by the linear first-order delay system with dead time in the continuous-time domain:

$$\Delta\tilde{o}(t) = K\left[1 - exp\left(-\frac{t-L}{T}\right)\right], \quad (1)$$

where K is proportional gain, T is time constant (s), and L is dead time (s). The parameters fitted to the step responses (averaged data: n = 5) in the DB or SN infusion were calculated by using least squares method and used to compute the unit impulse response.

The linear model response [$\Delta o^*(t)$] was calculated by the convolution integral in the discrete-time domain [9]:

This study was partly funded by a Grant-in-Aid for Scientific Research (C) from Japan Society for the Promotion of Science (KAKENHI, 25330171; 17K01297).

K. Kashihara is with Tokushima University, Minamijyousanjima 2-1, Tokushima, Japan (e-mail: kojikasi@is.tokushima-u.ac.jp).

$$\begin{cases} \Delta o^*(t) = \sum_{\tau=0}^{n} g(\tau)u(t-\tau)\,\Delta I & (2) \\ g(\tau) = \frac{K_u}{T} exp\left(-\frac{\tau - L}{T}\right), & (3) \end{cases}$$

where $u(.)$ is drug infusion rate (μg/kg/min), ΔI is sampling interval (s), and n is the finite number of terms in the model for the unit impulse response, $g(.)$, computed from the derived values of the step response. K_u is the proportional gain of the unit impulse response; T and L are the same values as in Eq. (1). For the simulation study, ΔI and n were set at 30 s and 20.

The unit impulse responses of ΔCO (ml/kg/min) and ΔAP (mmHg) during DB and SN infusions were determined by fitting the parameters to the average step responses (i.e., DB at 6 μg/kg/min and SN at 2 μg/kg/min). For the simulation study, the values of parameters K_u, T, and L were set as follows: K_u = 15.8, 4.4, 3.0, and -12.5; T = 164.3, 65.2, 40.6, and 209.4; L = 30, 30, 60, and 60 in the DB-CO, DB-AP, SN-CO, and SN-AP loops, respectively.

The $\Delta o^*(t)$ in Eq. (2) as the linear model response was modified by a sigmoidal function to express nonlinearity to a drug infusion:

$$\Delta o'(t) = p_1 tanh\left(\frac{p_2 \Delta o^*(t)}{2}\right), \quad (4)$$

where p_1 is the parameter of the response range showing the difference between the maximum and minimum values of $\Delta o'(t)$, and p_2 is the coefficient of gain; p_1 and p_2 were determined by nonlinear least squares method in the simulation study. Nonlinearity was calculated using the average values of the ΔCO and ΔAP responses in the final 30 s during DB (3, 6, and 9 μg/kg/min) and SN (1, 2, and 4 μg/kg/min) infusions for 10 min. The model parameters of the nonlinear-fitting functions in the simulation study were as follows: p_1 = 105.3, 22.8, 37.7, and -26.2; p_2 = 0.028, 0.145, 0.051, and -0.085 in the DB-CO, DB-AP, SN-CO, and SN-AP loops, respectively.

C. *Drug Interaction*

The drug interaction is expressed as follows:

$$\begin{cases} \Delta CO_M(t) = k_1 \Delta CO'_1(t) + k_2 \Delta CO'_2(t) \\ \Delta AP_M(t) = l_1 \Delta AP'_1(t) + l_2 \Delta AP'_2(t), & (5) \end{cases}$$

where $\Delta CO_M(t)$ is the model response with drug interactions of DB and SN; $\Delta CO_1'(t)$ and $\Delta CO_2'(t)$ are the nonlinear responses to DB and SN infusions, respectively; k_1 and k_2 indicate the proportional gain of the patient's sensitivity to DB and SN. In contrast, $\Delta AP_M(t)$ is the model's response to drug interactions of SN and DB; $\Delta AP_1'(t)$ and $\Delta AP_2'(t)$ indicate the nonlinear responses to SN and DB infusions, respectively; l_1 and l_2 are the proportional gains of sensitivity to SN and DB. For the simulation study, the values of the proportional gains (i.e., k_1, k_2, l_1, and l_2) were fixed at 1.

III. Methods for System Identification

A. *Convolutional Neural Networks*

CNN were used for the nonlinear system identification of the hemodynamics in heart failure patients during multiple drug infusions. For the simulation, the CNN structure was composed of three convolutional layers followed by two fully connected layers. In this study, an image (i.e., pixel values) describing the previous input-output data was applied to the input layer in the CNN (Fig. 1). The input/output values were temporarily normalized in order to learn the CNN. Here, the CNN component was separated in each target output (i.e., two inputs and single output) because the independent NN component in each output was previously shown to have effective results in nonlinear system identification [9].

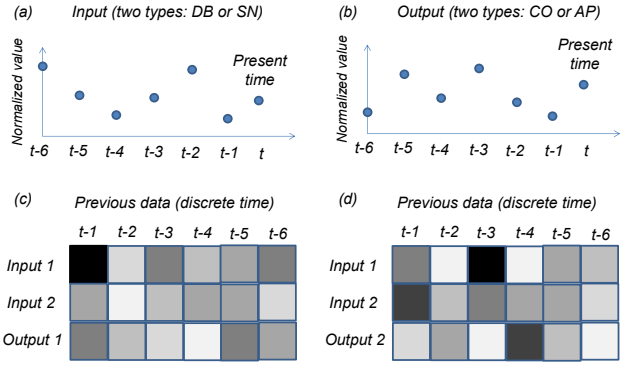

Fig. 1 (a) Input and (b) output data normalized for the CNN analysis. Examples of images in the input layer of CNN: the history of (c) CO or (d) AP responses to multiple drug infusions.

The convolution operation in each layer is described in the following equation:

$$Conv._i(\boldsymbol{Y}) = \max(0, \boldsymbol{W}_i * \boldsymbol{Y} + \boldsymbol{B}_i), \quad (6)$$

where $\boldsymbol{Y}$ is observed signals, $\boldsymbol{W}_i$ is filter kernels, $\boldsymbol{B}_i$ is biases, and * is the convolution operation. The convolutional layers can learn multiple filter kernels as feature maps. In this study, rectified linear unit (ReLU) was applied as the activation function to the output of the convolutional layers. The output of the convolutional layer corresponds to the input of the pooling layer, and the operation of the pooling layer provides a form of translation invariance. The final convolution layer is followed by fully connected layers.

The loss function in the learning process was the mean square error between the correct and CNN outputs. The Adam optimization algorithm was used to adjust the learning rate:

$$\vartheta_t = \vartheta_{t-1} - \alpha E[g]/\sqrt{E[g^2]}, \quad (7)$$

where θ is the learning parameter; α is the learning rate; g is the gradient; E is the expectation value.

2) Parameters of CNN: The size of the filter kernels was set at 3 × 3, which was obtained by the trial and error method, considering the input image size. There were 12 feature maps in each layer. The padding process prevented the reduction of the image size by image filtering. The max-pooling operation was also applied to each convolutional layer. In the fully connected layers, the number of elements was set at 8 in each layer. In the stochastic gradient descent learning algorithm, the mini-batch size was 20; the learning rate (α) was 0.001; the number of epochs was 200.

B. *Transfer Function Based on FFT Analysis*

The linear trend was subtracted from the input/output data. The FFT analysis was then performed to acquire the frequency spectra of the input and output signals. The input power [$S_{xx}(f)$], output power [$S_{yy}(f)$], and cross power between

input and output [$S_{yx}(f)$] were calculated, where f is frequency.

The transfer function [$G(f)$] from input to output can be computed as follows:

$$G(f) = S_{yx}(f)/S_{xx}(f). \quad (8)$$

The modulus [$|G(f)|$] and phase [$\theta(f)$] of the transfer function can be described in the following equations:

$$\begin{cases} |G(f)| = \sqrt{G_{Re}(f)^2 + G_{Im}(f)^2} & (9) \\ \vartheta(f) = \tan^{-1}[G_{Im}(f)/G_{Re}(f)] , & (10) \end{cases}$$

where $G_{Re}(f)$ and $G_{Im}(f)$ are the real and imaginary parts of $G(f)$, respectively. Modulus means dynamic gain.

In the following simulations, the nonparametric impulse response and the parametric auto-regressive exogenous input (ARX) model [$A(q)\, y(t) = B(q)\, u(t-n_k) + e(t)$, where q is the delay operator; $n_a = 2$ (number of poles); $n_b = 2$ (number of zeros plus 1); $n_k = 2$ (dead time)] were estimated from the transfer function based on above gain and phase. Here, please note that the linear system identification based on the FFT analysis must be generally performed using the single input and single output [11].

IV. Simulation Study for System Identification

A. *Evaluation Methods*

To carry out the dynamic system identification, the drug infusion rates of DB and SN as the system input were pseudo-randomly disturbed by limiting them between 0 and 10 μg/kg/min. The system output (i.e., CO and AP) were computed using the mathematical models that were defined in Section II. For all the analyses, the errors between actual and estimated values were calculated.

In the classical approaches to linear system identification, the nonparametric impulse response model and the parametric ARX model were used to predict responses. The accuracy of the NN was then compared with that of the CNN (see Section III for details) by using the same input/output data. The NN structure was composed of the two fully connected layers alone, without the convolutional layers in the CNN. The learning curves for the NN and the CNN were obtained from the training and test data for a single session.

B. *Simulation Results*

Fig. 2 indicates an example of output data during multiple drug infusions. The input data were randomized, and each output included the effects of two drug infusions (i.e., DB and SN). The observed time was 100 min; the nonlinear system identification was performed by using these data. For single-input single-output data (i.e., the DB-CO or SN-AP loop) without considering interactions, the prediction accuracies in the impulse response and the ARX model were as follows: 64.96% and 48.27% in the DB-CO loop; 36.81% and 17.22% in the SN-AP loop.

Fig. 3 shows the learning curve in the standard NN and the simulated response comparison between the correct and predicted outputs. The training loss converged to constant values of around 75 and 50 epochs in CO and AP, respectively. The average errors between the correct and predicted outputs in the standard NN were as follows: 5.68 ml/kg/min in CO and 1.23 mmHg in AP.

Fig. 4 shows the learning curve of the CNN and the predicted output. The single output (i.e., CO or AP) was estimated by the CNN with the inputs of multiple drugs (i.e., DB and SN). The CNN learning was completed at around 100 epochs in each target. Compared with the case of the standard NN, the predicted values were almost consistent with the correct outputs in CO (the error of 3.84 ml/kg/min) and AP (0.74 mmHg). However, when a significant change occurred (e.g., CO response around 70 × 0.5 min), the predicted value could not be followed up sufficiently.

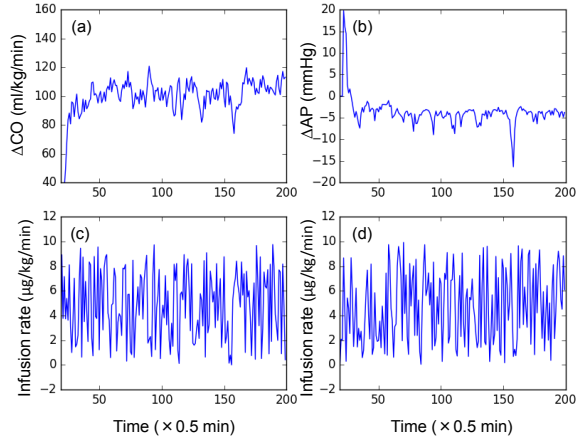

Fig. 2 Time-course data on the hemodynamics during multiple drug infusions. (a) CO and (b) AP outputs; (c) DB and (D) SN inputs.

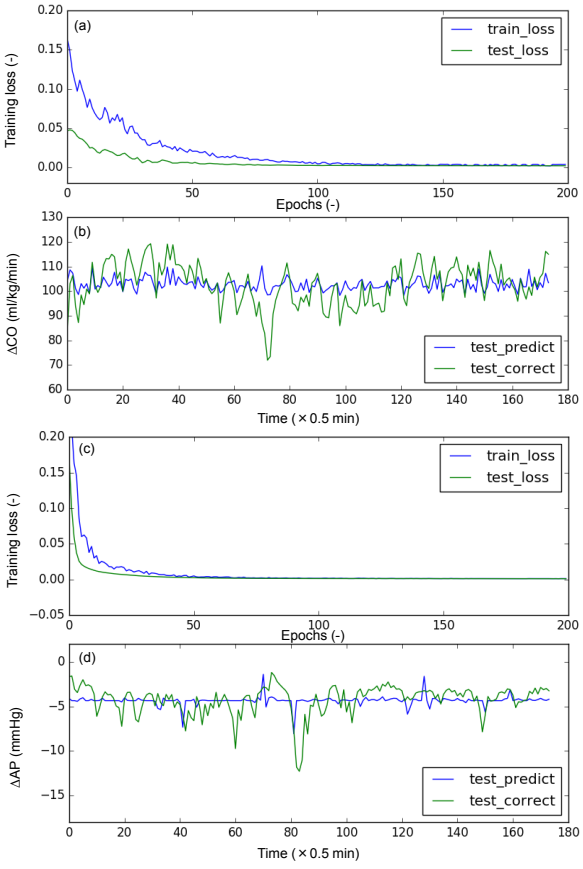

Fig. 3. The learning curve of NN: (a) CO and (c) AP outputs; the predicted output after the system identification: (b) CO and (d) AP.

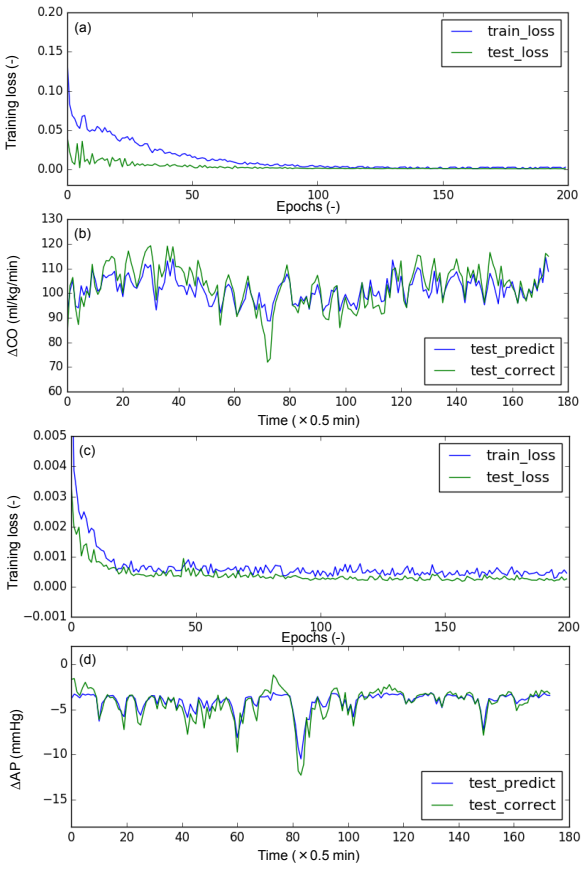

Fig. 4. The learning curve of CNN: (a) CO and (c) AP outputs; the predicted output after the system identification: (b) CO and (d) AP.

V. Discussion

In the simulation results, the CNN process showed the highest accuracy among all the methods tested in this study. The sufficiently learned CNN could have created the optimal feature maps to reflect the previous input/output history. In contrast, the system identification based on the FFT analysis assumed a linear time-invariant system [11]. Accordingly, the impulse response model and the ARX model showed the lowest simulation results of the predicted outputs under strong nonlinearity. Although the NN described the nonlinear characteristics, it may be difficult to consider complicated interactions among drug infusions (e.g., three or more drug infusions) because all the time-course data must be directly input to the fully connected layers of the NN.

The CNN structure should be appropriately set for the analysis of pharmacodynamics. Although the deep NN structure was also tested (unpublished data), the accuracy of the simulation results was not satisfactory. In addition, recurrent NN (e.g., long short-term memory: LSTM) can generally predict time-course data [12]. However, the results of the dynamic system identification may improve if the data on the input/output history are directly input to the NN [9]. In this situation, the input layer of the NN requires a large amount of input/output data. In contrast, the CNN can simply analyze such data as image information. Here, when the single output to multiple inputs is applied to the independent component of the CNN, the output prediction would become accurate. However, in future research, it should be determined whether a nonlinear dynamic system could be simultaneously identified by using an image with multiple inputs and outputs. In this case, the history of multiple inputs and outputs can be preserved as an image for the CNN input.

A mathematical model of the CO and AP responses to drug infusions may depend on the protocols of animal experiments. In addition, the simple model responses were used in this study; however, drug interactions vary in actual cardiac patients and hemodynamic responses are complicated by the use of multiple therapeutic agents. Therefore, further studies should be required, assuming clinical situations.

VI. Conclusion

The CNN structure with information on the input/output history of heart failure was designed; it was evaluated in simulations of nonlinear system identification of the CO and AP responses to DB and SN infusions under the existence of drug interactions. The results showed that the CNN were superior in obtaining the dynamical system characteristics compared with the results of the NN and the FFT analysis. Based on these results, the CNN could be applied in nonlinear dynamical system identification regardless of the complicated hemodynamic responses to drug infusions. Therefore, this method could be included in the optimal cardiac treatment with multiple therapeutic agents.

References

[1] O.A. Meretoja (1980) Influence of sodium nitroprusside and dobutamine on the haemodynamic effects produced by each other. Acta Anaesthesiol. Scand. 24:195–198

[2] J.S. Forrester, G. Diamond, K. Chatterjee, H.J. Swan (1976) Medical therapy of acute myocardial infarction by application of hemodynamic subsets (second of two parts). N Engl. J. Med. 295:1404–1413

[3] D.E. Mohrman, L.J. Heller (1997) Cardiovascular physiology, 4th ed. New York: McGraw-Hill

[4] R. Gopinath, B.W. Bequette, R.J. Roy, H. Kaufman, C. Yu (1995) Issues in the design of a multirate model-based controller for a nonlinear drug infusion system. Biotechnol. Prog. 11:318–332

[5] R.R. Rao, B. Aufderheide, B.W. Bequette (2003) Experimental studies on multiple-model predictive control for automated regulation of hemodynamic variables. IEEE Trans. Biomed. Eng. 50:277–288

[6] K.S. Narendra, K. Parthasarathy (1990) Identification and control of dynamic systems using neural networks. IEEE Trans. Neural Netw. 1:4–27

[7] Y. Takahashi (1993) Adaptive predictive control of nonlinear time-varying system using neural network. IEEE Int. Conf. Neural Netw. 3:1464–1468

[8] K. Kashihara, T. Kawada, K. Uemura, et al. (2004) Adaptive predictive control of arterial blood pressure based on a neural network during acute hypotension. Ann. Biomed. Eng. 32:1365–1383

[9] K. Kashihara (2006) Automatic regulation of hemodynamic variables in acute heart failure by a multiple adaptive predictive controller based on neural networks. Ann. Biomed. Eng. 34:1846–1869

[10] K. Kashihara (2016) Deep convolutional neural networks improve vein image quality, Proc. of 17th IEEE International Symposium on Computational Intelligence and Informatics (CINTI 2016), 209–212

[11] K. Kashihara (2015) Dynamically assessing the arterial baroreflex by examining ramp responses to vasoactive agents, Proc. of 2015 IEEE/SICE International Symposium on System Integration, 965–970

[12] N. Laptev, J. Yosinski, L.E. Li, S. Smyl (2017) Time-series extreme event forecasting with neural networks at uber. In International Conference on Machine Learning.